Received: 8 April 2022 | Revised: 10 June 2022 | Accepted: 17 June 2022

DOI: 10.1111/1462-2920.16107

RESEARCH ARTICLE

environmental microbiology sfam

Polar flagellar wrapping and lateral flagella jointly contribute to *Shewanella putrefaciens* environmental spreading

Marco J. Kühn[1,2] | **Daniel B. Edelmann**[1] | **Kai M. Thormann**[1]

[1]Institut für Mikrobiologie und Molekularbiologie, Justus-Liebig-Universität Gießen, Gießen, Germany

[2]Institute of Bioengineering and Global Health Institute, School of Life Sciences, École Polytechnique Fédérale de Lausanne, Lausanne, Switzerland

Correspondence
Kai M. Thormann, Institut für Mikrobiologie und Molekularbiologie, Heinrich-Buff-Ring 26-32, 35392 Gießen, Germany.
Email: kai.thormann@mikro.bio.uni-giessen.de

Funding information
Deutsche Forschungsgemeinschaft, Grant/Award Numbers: TH 831/6-1, TH 831/8-1

Abstract

Flagella enable bacteria to actively spread within the environment. A number of species possess two separate flagellar systems, where in most cases a primary polar flagellar system is supported by distinct secondary lateral flagella under appropriate conditions. Using functional fluorescence tagging on one of these species, *Shewanella putrefaciens*, as a model system, we explored how two different flagellar systems can exhibit efficient joint function. The *S. putrefaciens* secondary flagellar filaments are composed as a mixture of two highly homologous non-glycosylated flagellins, $FlaA_2$ and $FlaB_2$. Both are solely sufficient to form a functional filament, however, full spreading motility through soft agar requires both flagellins. During swimming, lateral flagella emerge from the cell surface at angles between 30° and 50°, and only filaments located close to the cell pole may form a bundle. Upon a directional shift from forward to backward swimming initiated by the main polar flagellum, the secondary filaments flip over and thus support propulsion into either direction. Lateral flagella do not inhibit the wrapping of the polar flagellum around the cell body at high load. Accordingly, screw thread-like motility mediated by the primary flagellum and activity of lateral flagella cumulatively supports spreading through constricted environments such as polysaccharide matrices.

INTRODUCTION

Being motile provides a huge advantage for many bacteria (Fenchel, 2002; Reichenbach et al., 2007). For locomotion many species employ flagella, which mediate a very efficient means of motility within liquids or across surfaces (Jarrell & McBride, 2008; Kearns, 2010; Wadhwa & Berg, 2021). Flagella are long proteinaceous filaments that have a helical geometry and can be engulfed by a membrane, the so-called sheath, or decorated by glycosylation (Chu et al., 2020; Merino & Tomás, 2014; Nakamura & Minamino, 2019). These helical filaments are rotated at the filament's base by the membrane-embedded flagellar motor, which results in a highly efficient propulsion. Motor activity depends on ion gradients with H^+ or Na^+ as most common coupling ions (Biquet-Bisquert et al., 2021). Most flagellar motors are bidirectional and allow clockwise (CW) and counterclockwise (CCW) rotation (Nakamura & Minamino, 2019), and this alternation commonly leads to reorientation of the cell body, thereby changing the direction of swimming. In the majority of bacteria, the motor behaviour is controlled by one or more associated chemotaxis systems, which perceive environmental signals and convert them into the phosphorylation state of the response regulator CheY, which then binds to the flagellar motor(s) to induce directional switches (Bi & Sourjik, 2018). By controlling the run lengths between directional switches, the cells can perform a so-called biased

random walk to move towards favourable and away from non-favourable environments (Sourjik & Wingreen, 2012).

Bacterial flagellation comes in two main patterns: Species such as *Escherichia coli* and *Bacillus subtilis* have a peritrichous flagellation pattern with several flagella originating from lateral positions of the cell body (Berg, 2004; Najafi et al., 2018; Schuhmacher et al., 2015). In contrast, many bacteria are flagellated at one or both cell poles (such as species of the genus *Caulobacter*, *Vibrio*, *Pseudomonas*, *Shewanella*, *Helicobacter*, *Agrobacterium*, *Azospirillum*, to name just a few) with one or more individual flagellar filaments. This has profound consequences for the mechanism of propulsion and directional switches/navigation (Thormann et al., 2022). *Escherichia coli* moves by the paradigm run-tumble pattern (Berg, 2004): when the filaments rotate in CCW direction, the flagella form a bundle pushing the cells forward. Upon switch of one or more motors to CW rotation, the corresponding filament(s) will leave the bundle, leading to a realignment of the cell body. Upon re-switching to CCW rotation, the cell will continue into a new direction. In contrast, many monopolarly flagellated bacteria, such as *Vibrio alginolyticus* or *Shewanella putrefaciens*, navigate by a different mechanism: CCW rotation of the left-handed flagellar helix pushes the cell forward, while CW rotation pulls the cell backward. Re-switching to CCW rotation and pushing of the cell results in compression of the structure connecting filament and motor, the flagellar hook, which leads to a quick realignment of the cell, referred to as 'run-reverse-flick' (Bubendorfer et al., 2014; Son et al., 2013; Xie et al., 2011).

Notably, a number of polarly flagellated bacterial species (including but not restricted to the genera *Aeromonas*, *Azospirillum*, *Bradyrhizobium*, *Rhodospirillum*, *Shewanella*, *Vibrio*) harbour a separate secondary lateral flagellar system in addition to the main polar flagellum (Bubendorfer et al., 2012; Jiang et al., 1998; Kanbe et al., 2007; Kawagishi et al., 1995; McClain et al., 2002; Shimada et al., 1985; Shinoda & Okamoto, 1977). Studies on these systems provided evidence that formation of lateral flagella is induced under specific environmental conditions (such as nutrients, surface contact or increased viscosity), which in turn improves motility, enables swarming across surfaces or benefits attachment to biotic surfaces (McCarter, 2004; Merino et al., 2006). Thus, these cells operate two different flagellar systems in parallel. Little is known about the properties of secondary lateral flagella, how they cooperate with the primary system and how they impact the swimming behaviour.

One representative species harbouring such a dual flagellar system is *Shewanella putrefaciens*. In previous studies we showed that this species is mainly propelled by a single polar flagellum with a left-handed helix, which is powered by Na^+ ions (Bubendorfer et al., 2012). The filament is modified by glycosylation and mediates free swimming and chemotactic navigation by a run-reverse-flick pattern (Bubendorfer et al., 2014; Kühn et al., 2017, 2018). In addition, we demonstrated that, at high load on the flagellum, the filament can wrap around the cell body to allow backward transition in a screw thread-like fashion (Kühn et al., 2017). This mode of motility is particularly effective close to or in contact with a substratum and is thought to be a means of escaping from traps or dead ends, which cells will encounter when moving through structured environments such as polysaccharides (mucus, slime, the matrix of biofilms) or the narrow channels of soils and sediments. The filament consists of two major building blocks, the flagellins FlaA and FlaB, in a spatial arrangement that stabilizes the filament to suppress the flagellar wrapping and screw thread motility during free swimming (Kühn et al., 2018).

The secondary flagellar system of *S. putrefaciens* is induced in complex media and in structured soft agar, leading to a subpopulation of cells with one or more lateral flagella in addition to the main polar filament (Bubendorfer et al., 2012). During mid-exponential phase in LB media, some 10% of the cells exhibit secondary flagellation (Bubendorfer et al., 2012), while almost all cells at the outer fringes of soft-agar spreading zones are equipped with primary and secondary filaments (Bubendorfer et al., 2014). Expression of the secondary flagellar system depends on the phosphodiesterase PdeB and therefore likely on c-di-GMP levels (Rossmann et al., 2019). In contrast to the polar system, the lateral flagella are H^+-driven and not addressed by the chemotaxis system due to the absence of the CheY-binding site at the flagellar motor (Bubendorfer et al., 2014). As a consequence, the lateral flagella only turn CCW. However, the rotational speed can be regulated via the c-di-GMP-binding protein MotL (Pecina et al., 2021). Wild-type cells with polar and lateral flagella outperformed exclusively monopolarly flagellated mutants in spreading through soft agar and during free swimming. This could not be attributed to an increase in swimming speed but is thought to be at least partly due to an effect of the additional filaments on the cells' turning angles and run lengths, resulting in a higher directional persistence (Bubendorfer et al., 2014).

Here we further studied the formation and behaviour of the secondary lateral flagellar filaments of *S. putrefaciens* in concert with the primary polar filament. By flagellin labelling and fluorescence microscopy we show that the secondary flagella are assembled by a mixture of two distinct flagellins resulting in left-handed filaments, which act as a support for the primary polar flagellum during movement in both forward and backward directions. In addition, polar flagellar wrapping and lateral flagellar function increase the ability of

S. putrefaciens to spread through structured environments in a cumulative fashion.

EXPERIMENTAL PROCEDURES

Bacterial strains, growth conditions and media

All bacterial strains used in this study are summarized in Supplementary Table 1. *Shewanella* cells were grown in LB medium at room temperature or 30°C, cells of *Escherichia coli* in LB medium at 37°C. Media for *E. coli* WM 3064 [2,6-diaminoheptanedioic acid (DAP)-auxotroph] were supplemented with DAP at a final concentration of 300 μM. Selective media were supplemented with 50 mg ml^{-1} kanamycin and/or 10% (wt. $vol.^{-1}$) sucrose when appropriate. Solid media were prepared by adding 1.5% (wt. $vol.^{-1}$) agar. To perform growth experiments, overnight cultures of *S. putrefaciens* were diluted into fresh LB medium to yield a final OD_{600} of 0.01. 200 μl of the diluted culture was incubated at 30°C under continuous shaking in an EPOCH2 microplate reader (BioTek) using the Gen5 software (3.10.06, BioTek). OD measurements were performed at intervals of 5 min.

Soft-agar spreading assay

Semi-solid LB medium was prepared by supplementing with 0.15%–0.25% (wt. $vol.^{-1}$) select agar (Invitrogen), boiling and subsequent cooling to 30°C–40°C before pouring into square Petri dishes of appropriate size. After solidification, 2 μl of exponentially grown cultures were spotted on the plates and incubated in a moist environment overnight at room temperature. Plates were scanned using an Epson V700 Photo Scanner before the spreading halos could merge. For direct comparison, different strains were always incubated on the same plate. Swimming/spreading ability was measured as relative diameters compared to that of wild-type cells or other appropriate reference strains.

Strains and vector constructions

Plasmids and corresponding oligonucleotides used in this study are summarized in Supplementary Tables 2 and 3, respectively. Gene deletions and insertions strains were generated by sequential double homologous recombination using the suicide plasmid pNPTS-R6K (Lassak et al., 2013). Briefly, substitution fragments were constructed by combining approximately 500-bp fragments of the up- and downstream regions of the designated gene. For gene deletions a few codons (typically around six) were kept to prevent disruption of regulatory elements of neighbouring genes. In-frame insertions were constructed and re-integrated into corresponding deletion strains similarly. Single or multiple nucleotide substitutions were done by inserting a modified gene fragment into the corresponding gene deletion. Plasmids were constructed using standard Gibson assembly protocols (Gibson et al., 2009) and transferred into *Shewanella* cells by conjugative mating with *E. coli* WM3064.

RNA isolation and qRT-PCR

Total RNA was isolated from exponentially growing *Shewanella* cells ($OD600 = 0.4$) using a Direct-zol RNA MiniPrep (Zymo Research) according to the manufacturer's instructions. RNA concentrations were measured at 260 nm. Residual DNA was removed with a Turbo DNA-free Kit (Thermo Fisher Scientific) according to the manufacturer's instructions. RNA samples were stored at −80°C. qRT-PCR was performed with a C1000 Thermal Cycler using theCFX96 Real-Time System (Bio-Rad) and low-profile strips with ultraclear caps (Thermo Fisher Scientific). PCR amplification was carried out using a Brilliant III Ultra-Fast SYBR® Green QRT-PCR Master Mix (Agilent Technologies) in a 10 μl reaction volume and 1 ng μl^{-1} final RNA concentration according to the manufacturer's instructions. Cycling conditions were as follows: a reverse-transcription step at 50°C for 10 min and 95°C for 3 min, then 40 cycles of 95°C for 5 s and 60°C for 10 s. The cycle threshold (Ct) was determined automatically after 40 cycles (Real-Time CFX Manager 2.1, Bio-Rad). Ct values for $flaAB_2$ (Sputcn32_3456 and Sputcn32_3455) were normalized against the Ct value of *gyrA* (Sputcn32_2070). Two-tailed Welch's *t*-test was performed to test for statistical differences.

Flagellar filament staining and microscopy

Surface-exposed threonine residues of the flagellin monomers were substituted with cysteine residues and selectively labelled with maleimide-ligated fluorescent dyes as previously described (Kühn et al., 2017). To verify that cysteine substitutions within the flagellin did not affect the swimming behaviour negatively we performed soft agar swimming assays and Western blot analyses. For visualization by microscopy, cells were either harvested from an exponential culture (OD_{600} of around 0.6) or, to enrich cells that produce lateral flagella, from the outer fringes of a colony spreading on a soft-agar plate (0.3% select agar). Cells were sedimented by centrifugation (1200*g*, 5 min, room temperature) and resuspended in 50 μl PBS. To prevent shearing off flagellar filaments, pipette tips were always cut off when pipetting cells. 1 μl CF™ 488 maleimide (Sigma-

Aldrich) was added and the cell suspension was incubated in the dark for 15 min. To remove residual unbound dye, cells were centrifuged and carefully washed with 1 ml of PBS. Finally, cells were resuspended in LM100 medium [10 mM HEPES, pH 7.3; 100 mM NaCl; 100 mM KCl; 0.02% (wt. vol.$^{-1}$) yeast extract; 0.01% (wt. vol.$^{-1}$) peptone; 15 mM lactate] and used for microscopy within 30 min. Typically, 150–300 frames were recorded at 20–50 ms exposure time. Microscopy was performed at room temperature using a custom microscope setup (Visitron Systems) based on a Leica DMI 6000 B inverse microscope (Leica) equipped with a pco.edge sCMOS camera (PCO), a SPECTRA light engine (lumencor) and an HCPL APO 63×/1.4–0.6 objective (Leica) using a custom filter set (T495lpxr, ET525/50m; Chroma Technology).

Determining flagellar helix parameters

To measure the pitch, diameter and axis length of the secondary flagella cells were prepared as described above and several images close to the glass coverslip were taken. Parameters were measured manually using the ImageJ distribution Fiji (Schindelin et al., 2012). Only flagella with a homogenous shape were considered. The handedness of flagellar filaments was determined by recording z-stack sequences which show characteristic patterns for left-handed and right-handed helices. We identified the handedness of secondary flagellar filaments as left-handed.

Determination of swimming speed

To determine the swimming speed of *Shewanella* strains, cells were cultured in LB with 0.25% (wt. vol.$^{-1}$) select agar (Invitrogen) overnight. Cultures were washed out of the agar using 1× PBS and diluted to reach an OD_{600} of ~0.3. Microscopy image series were recorded at 50 ms time intervals and analysed using the TrackMate (v7.6.1) Fiji ImageJ plugin (Tinevez et al., 2017).

Protein separation and Western blotting

Cells were grown in LB medium until exponential phase (OD_{600} around 0.5). Cell lysates were obtained by centrifuging cells corresponding to an $OD_{600} = 10$ and resuspending the cell pellet in Laemmli buffer (Laemmli, 1970). Samples were heated to 95°C for 5 min and proteins were separated by SDS/PAGE using 12% (wt./vol.) polyacrylamide gels. Subsequently, the proteins were transferred to a nitrocellulose Roti-PVDF membrane (Roth) by semidry transfer. The secondary flagellins $FlaA_2$ and $FlaB_2$ of *S. putrefaciens* were detected using polyclonal antibodies (dilution 1:1000) which were raised against the secondary flagellins (Eurogentec Deutschland). Anti-rabbit IgG-horseradish peroxidase (Thermo Fisher Scientific, prod. # 31460) was used as secondary antibody (dilution 1:20,000). The horseradish peroxidase signal was detected with the CCD System LAS 4000 (Fujifilm) after incubation with SuperSignalH West Pico Chemiluminescent Substrate (Thermo Scientific) for 0.5–1 min.

Statistics of filament parameters

Pitch, diameter and flagellar axis length of 50 cells were measured. The actual length of the filament (arc length) was calculated from the obtained parameters. Significance was tested with a two-sided two-sample *t*-test or Welch's *t*-test ($p < 0.01$, Bonferroni corrected) in R version 4.1.3.

RESULTS

Composition of the lateral flagellar filaments

Bacterial flagellar filaments are mainly composed of the building block flagellin. According to the *Shewanella putrefaciens* CN-32, henceforth *S. putrefaciens*, genome data, two neighbouring flagellin-encoding genes, $flaA_2$ (Sputcn32_3456) and $flaB_2$ (Sputcn32_3455) are present within the gene cluster [Figure 1(A)], which encodes the complete lateral flagellar system (Bubendorfer et al., 2012). Although $flaB_2$ is directly located downstream of $flaA_2$, the two genes are separated by a gap of 237 bp including a predicted putative Rho-independent terminator structure, suggesting that both genes are transcribed separately. The encoded flagellins consist of 267 ($FlaA_2$) and 270 ($FlaB_2$) amino acids and have predicted molecular masses of 27.6 ($FlaA_2$) and 27.9 kDa ($FlaB_2$). The two proteins are highly homologous (87% identity, 88% similarity; Supplementary Figure 1). The vast majority of the differences in the amino acid sequences occur in the variable region outside of the D0-D1 regions, which mediate the stacking of the flagellins in the filament.

We previously showed that the primary polar filament of *S. putrefaciens* CN-32 is assembled from two distinct flagellins, $FlaA_1$ and $FlaB_1$ (Sputcn32_2586 and Sputcn32_2585), in a spatially organized fashion: $FlaA_1$ is predominantly forming a segment at the base of the filament close to the cell body, while the major distal part (>80%) of the filament is almost exclusively composed of $FlaB_1$ (Kühn et al., 2018). We therefore determined if the secondary flagella are similarly assembled from both $FlaA_2$ and $FlaB_2$. To answer this

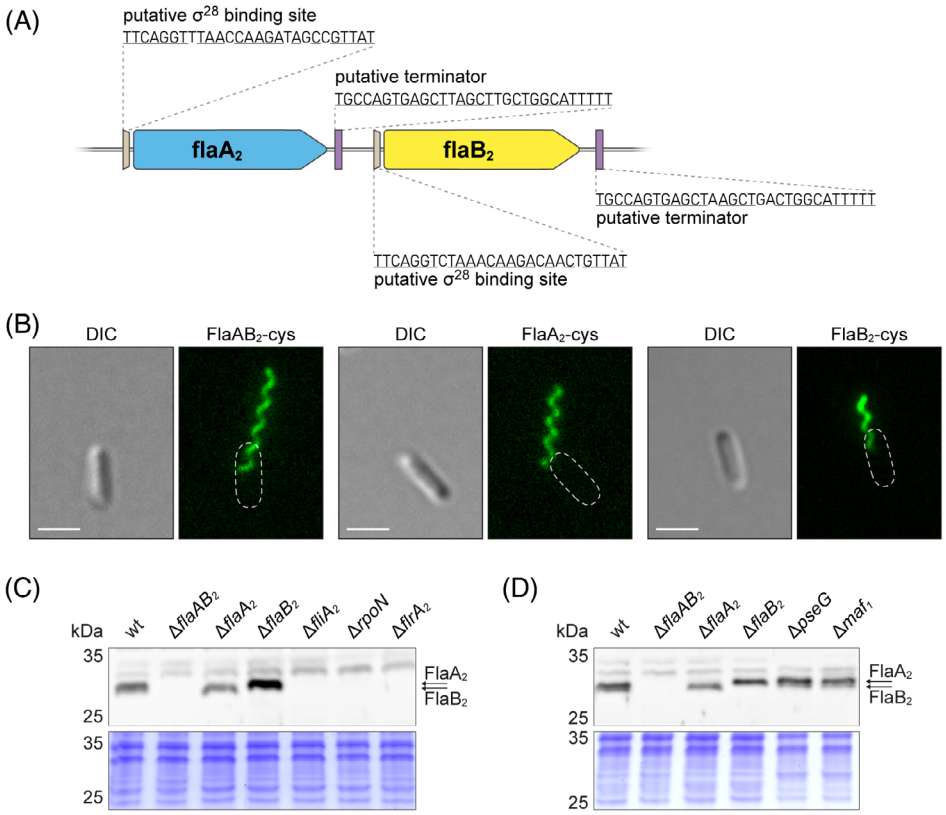

FIGURE 1 Genetic organization and properties of the *S. putrefaciens* secondary flagellins. (A) Genetic organization of *flaA*$_2$ and *flaB*$_2$. Each gene is predicted to possess a σ^{28} binding site within the promoter region and a downstream transcriptional terminator structure. σ^{28} binding sites were predicted based on the previously identified consensus sequence (Song et al., 2007, 2008). Terminators were predicted by ARNold (Gautheret & Lambert, 2001; Macke et al., 2001). Both σ^{28} binding sites and terminator structures are highly similar as indicated by underlining identical bases. (B) Micrographs of cells with fluorescently labelled secondary flagellar filaments (FlaAB$_2$-cys). Individual labelling [FlaA$_2$-cys (middle panels) and FlaB$_2$-cys (right panels)] revealed that both flagellins are present throughout the whole filament. Both flagellins are solely sufficient to assemble a functional filament (also see Supplementary Figures 2 and 3). Scale bars represent 2 μm. (C, D) Western blotting analyses of the secondary flagellins in various deletion strains. Upper panels = immunoblots, lower panels = corresponding Coomassie-stained PAGE loading controls. (C) FlaA$_2$ and FlaB$_2$ can be discriminated by their molecular mass. Expression of both flagellins requires σ^{54} and σ^{28} (RpoN and FliA$_2$, respectively) as well as the major regulator of secondary flagellar assembly FlrA$_2$. (D) The apparent mass of both secondary flagellins does not change in strains deleted in two major glycosylation proteins, Maf1 and PseG, indicating that the secondary flagellins are not modified by glycosylation

question, we selectively labelled the flagellins to visualize the amount and position within the filament by fluorescent microscopy. To this end, we genetically substituted threonine residues of FlaA$_2$ and/or FlaB$_2$ within the variable region with cysteine, which allowed coupling of fluorescent maleimide dyes to assembled flagellar filaments. Substituting T159 and T160 to C in FlaA$_2$ (FlaA$_{2\ T159C\ T160C}$; FlaA$_2$-Cys) and/or T159 and T162 to C in FlaB$_2$ (FlaB$_{2\ T159C\ T162C}$; FlaB$_2$-Cys) resulted in secondary flagellar filaments that were highly fluorescent after fluorescent labelling. The mutated secondary filaments also supported normal flagella-mediated spreading through soft agar [Supplementary Figure 2(A)], indicating that the substitutions within the flagellin do not interfere with the flagellar function.

Fluorescent microscopy revealed that in flagellar filaments in which only FlaA$_2$-Cys or FlaB$_2$-Cys were labelled, the fluorescence always occurred throughout the full length of the filament [Figure 1 (B)]. This pattern strongly indicated that both flagellins are used to assemble the secondary flagella and that, as opposed to the primary flagellum, there is no specific spatial arrangement of FlaA$_2$ and FlaB$_2$ within the secondary filaments. The secondary filaments had a variable length from 3 to 8 μm and exhibited a left-handed helix with a diameter of about 0.4 μm and a pitch of about 1 μm (Supplementary Figure 3).

FlaA2 and FlaB2 are solely sufficient to form a functional secondary flagellar filament

In Gram-negative bacteria, flagellin-encoding genes are often controlled by a dedicated alternative sigma factor, which initiates transcription once the hook, the

structure that connects basal body and flagellar filament, is completed (Chevance & Hughes, 2008). Previous studies showed that in the primary system, only *flaB*$_1$ is under control of this alternative sigma factor, FliA$_1$. This leads to sequential production and export of FlaA$_1$ and FlaB$_1$, which results in the observed spatial arrangement in the filament (Kühn et al., 2018). However, the assembly of the secondary filaments by two apparently equally distributed flagellins indicated a significantly different regulation pattern. Accordingly, potential FliA (σ^{28}) consensus sequences were predicted upstream of both *flaA*$_2$ and *flaB*$_2$ [see Figure 1(A)]. Furthermore, the secondary flagellar gene cluster includes a gene encoding an orthologue to the alternative sigma factor, FliA$_2$ (Sputcn32_3449). To determine if *flaA*$_2$, *flaB*$_2$ or both are under transcriptional control of FliA$_2$, *fliA*$_2$ was deleted (Δ*fliA*). Subsequently, production of FlaA$_2$ and FlaB$_2$ was detected by western blotting using antibodies raised against the conserved D$_0$–D$_1$-domains of the secondary flagellins [Figure 1(C)]. Both flagellins were readily detected in the presence but not in the absence of FliA$_2$, indicating that FlaA and FlaB are synchronously produced and exported, which leads to the observed equal distribution within the filament.

The formation of the filament with equally distributed FlaA$_2$ and FlaB$_2$ raised the question about the role of each flagellin in the filament's geometry. We therefore constructed mutants that assemble the flagellar filament using only one of the flagellins. To this end, we deleted either *flaA*$_2$ or *flaB*$_2$ from the chromosome, resulting in strains Δ*flaA*$_2$ *flaB*$_2$-*Cys* and *flaA*$_2$-*Cys* Δ*flaB*$_2$ that allowed fluorescent labelling of the residual flagellin. Both mutants assembled flagellar filaments that were barely distinguishable from wild-type lateral flagella with respect to the overall geometry of the filaments, e.g. handedness, diameter and pitch. However, the filaments of the mutants were, on average, somewhat shorter (∼5.8 μm, wild type; ∼5.0 μm, Fla$_2$-only; ∼4.2 μm, FlaB$_2$ only; Supplementary Figure 3). However, spreading mediated by the mutant lateral flagella was slightly but significantly decreased [FlaA$_2$-only by 12%; FlaB$_2$-only by 7%, Supplementary Figure 2(B)] compared to spreading mediated by wild-type lateral filaments consisting of both flagellins. We found that this difference could not be attributed to differences in swimming speed (mediated by the secondary flagella only, Supplementary Figure 4) or growth of the corresponding mutants (Supplementary Figure 5). Thus, the presence of either flagellin is sufficient to form a functional flagellar filament but full length and functionality, at least for spreading in soft agar, require both flagellins.

According to the western blot analysis [Figure 1 (C,D)], FlaA$_2$ appears to be produced in higher amounts than FlaB$_2$, To determine whether this was due to different expression of the corresponding genes, we performed qRT-PCR analysis and quantified the mRNA levels of *flaA*$_2$ and *flaB*$_2$ in strains in which the other secondary flagellin gene was deleted (Δ*flaAB*$_1$ Δ*flaB*$_2$ for quantification of *flaA*$_2$ expression and Δ*flaAB*$_1$ Δ*flaA*$_2$ for quantification of *flaB*$_2$ expression). We found that the expression levels of both genes were highly similar (Supplementary Figure 6), thus, the different amounts of flagellins are unlikely to be due to differences in expression, but may rather be related to differences in translation efficiency or protein stability. Notably, FlaA$_2$-only secondary filaments are shorter than wild-type and FlaB$_2$-only secondary filaments, indicating that the amount of the flagellins produced does not correlate with the length of the filaments.

FlaA2 and FlaB2 are not modified by glycosylation

The primary flagellar filaments of *S. oneidensis* and *S. putrefaciens* are decorated by glycosyl groups, which is required for proper assembly and normal flagellar function (Bubendorfer et al., 2013; Kühn et al., 2018; Sun et al., 2013). As flagellin glycosylation can also be observed for secondary flagella, e.g. in *Aeromonas hydrophila* (Canals et al., 2007; Gavín et al., 2003; Rabaan et al., 2001), we determined if the secondary flagellins of *S. putrefaciens* are similarly glycosylated and if this is related to their function. For the primary flagellins, glycosylation leads to pronounced upshifts in the position during separation in polyacrylamide gels, which would correspond to a much higher molecular mass than that deduced from the amino acid sequence (Bubendorfer et al., 2013; Kühn et al., 2018). In contrast, during PAGE separation both FlaA$_2$ and FlaB$_2$ migrate at positions according to their predicted molecular mass (about 28 kDa). In addition, we determined potential migration shifts of the secondary flagellins in mutants lacking *maf-1* or *pseG*, whose gene products were shown to be involved in glycosylation of the *S. putrefaciens* primary flagellins (Kühn et al., 2018). Loss of both genes did not result in a significant difference in the apparent molecular mass after PAGE separation and Western blotting [Figure 1(D)]. The results suggest that the secondary flagellins FlaA$_2$ and FlaB$_2$ may not be glycosylated by the same system acting on the polar system.

Behaviour of primary and secondary flagella during swimming

While the flagella filament behaviour during swimming in polarly and peritrichously flagellated bacteria has been characterized microscopically for some species, nothing is known about how a polar and a

lateral flagellar system jointly drive motility of a bacterial cell. To determine the flagellar behaviour, we combined the serine to cysteine substitution within the primary and secondary flagellins, which enabled synchronous labelling of the filaments of both flagellar systems (strain $FlaA_1B_{1Cys}$ $FlaA_2B_{2Cys}$). Cells expressing both flagellar systems were previously demonstrated to spread faster through soft-agar networks (Bubendorfer et al., 2014). Therefore, to enrich for cells with both flagellar systems active, samples were taken from the outer spreading areas on soft-agar plates. Subsequently, the flagellar filaments were fluorescently labelled, and the cells were used for time-lapse microscopy.

In agreement with previous studies, we typically observed cells with one to five secondary flagella in addition to the primary polar flagellum (Bubendorfer et al., 2012, 2014). As expected, the secondary filaments localized randomly at positions ranging from mid-cell to almost polar. Close to thousand of cells were observed with respect to behaviours of the flagellar filaments and how they impact the motion of corresponding cell. To this end, we focused on cells with clearly distinguishable primary and secondary flagella. Of note, the variations in secondary flagellar numbers and positioning result in a vast array of different flagellation arrangements and corresponding differences in individual behaviour of the cells. We therefore aimed to identify and highlight the representative flagellar filaments' behaviours and cell manoeuvres, which will be described in the following.

We generally observed that secondary filaments that were apparently positioned away from the cell pole never formed a bundle during swimming, as opposed to the *E. coli* paradigm. Instead, the secondary filaments pointed away from the cell surface at an angle of about 30°–50° towards the trailing end of the cell, both during pushing [forward swimming; Figure 2(A), Supplementary Movie M1] as well as during pulling [backward swimming; Figure 2(B), Supplementary Movie M2] mediated by the primary polar flagellum. In contrast, secondary flagella that were positioned close to the cell pole were able to align with the cell length axis. This was observed when one or more filaments were located at the pole opposite from the primary polar flagellum with the latter pulling the cell [Figures 2(B) and 3(A), Supplementary Movies M2 and M3] or, vice versa, when the secondary filaments occurred at the same pole as the primary filament with the latter pushing the cell [Figure 3(B); Supplementary Movie M4]. Under the latter conditions the secondary filaments may form bundles that may potentially also include the primary filament; however, this could not be unequivocally determined at the resolution obtainable during high-speed microscopy. The bundle-like structure would fall apart upon a directional switch induced by the main polar flagellum: The filaments within the potential bundle at the—now leading—cell pole would flip back at an angle probably restricted by the pole curvature, while the main polar flagellum would maintain its position pointing away from the cell pole [Figure 3(A), Supplementary Movie M3].

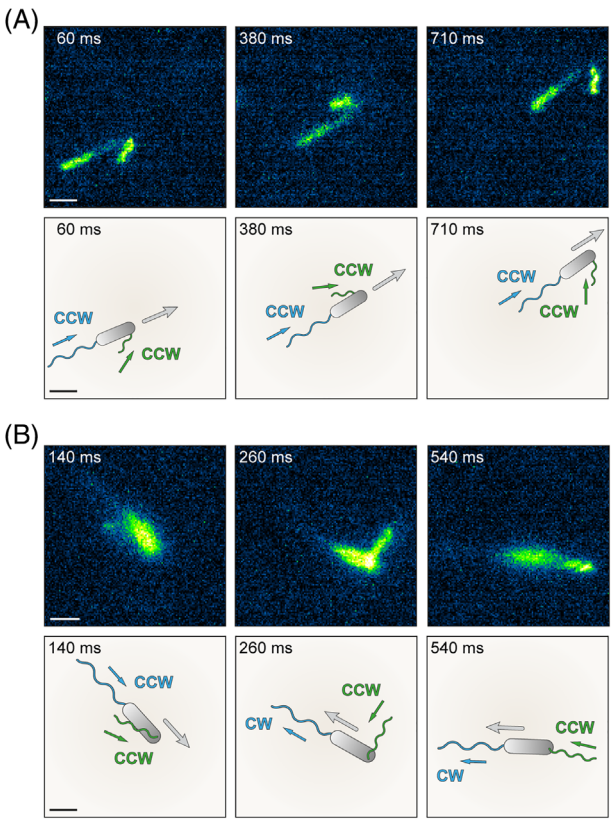

FIGURE 2 Localization-dependent secondary flagella behaviour. The figure shows snapshots of swimming *S. putrefaciens* cells with fluorescently labelled primary and secondary flagella and corresponding cartons illustrating the micrographs. Grey arrow, overall swimming direction of the cell. Blue/green arrows, direction of flagellar propulsion. CCW, counter-clockwise. CW, clockwise. Scale bar, 2 μm. (A) The cell is propelled forward by a polar flagellum rotating CCW (blue). The secondary lateral flagellum at the leading cell pole (green) points away from the cell surface towards the trailing cell pole and thus supports the forward propulsion of the primary flagellum. Snapshots were taken from Supplementary Movie M1. (B) During a reversal induced by the switch from CCW to CW motor rotation of the primary flagellum, the secondary flagellum flips over and continues supporting the propulsion of the primary flagellum as it always rotates CCW. During the reversal, the leading cell pole becomes the trailing cell pole where the secondary flagellum is located. This allows the secondary flagellum to align better with the cell length axis and in turn increases the propulsion efficiency as the thrust vectors of both primary and secondary flagella align. Snapshots were taken from Supplementary Movie M2

Irrespective of their position close to or away from the cell pole, the lateral flagella always flipped over without apparent changes of the handedness, morphology or direction of rotation. Thus, by the constant CCW rotation of the left-handed helix, the

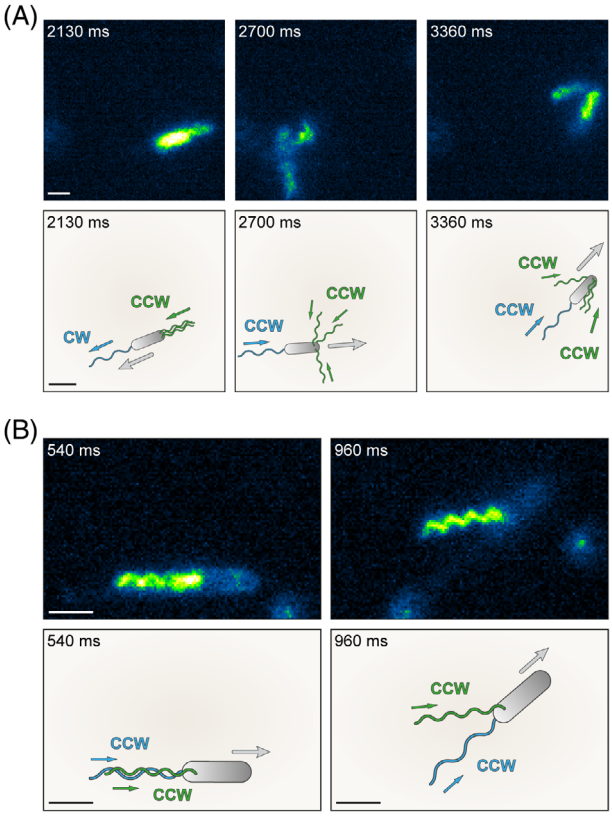

FIGURE 3 Secondary flagella may form a bundle when aligned behind the trailing cell pole. The figure shows snapshots of swimming *S. putrefaciens* cells with fluorescently labelled primary and secondary flagella and corresponding cartons illustrating the micrographs. CCW, counter-clockwise. CW, clockwise. Grey arrow, overall swimming direction of the cell. Blue/green arrows, direction of flagellar propulsion. Scale bar, 2 μm. (A) Secondary flagella (green) may form a bundle while being aligned and in close proximity behind the trailing cell pole. Upon reversal induced by the primary flagellum (blue) they flip over and point away from the cell surface in different directions. As secondary flagella always rotate CCW and get realigned during reversals due to viscous drag they always support the propulsion generated by the primary flagellum. Snapshots were taken from Supplementary Movie M3. (B) One primary and one secondary flagellum may form a bundle as long as they are aligned. The potential bundle falls apart once the cell turns and the secondary flagellum is dragged behind. Snapshots were taken from Supplementary Movie M4

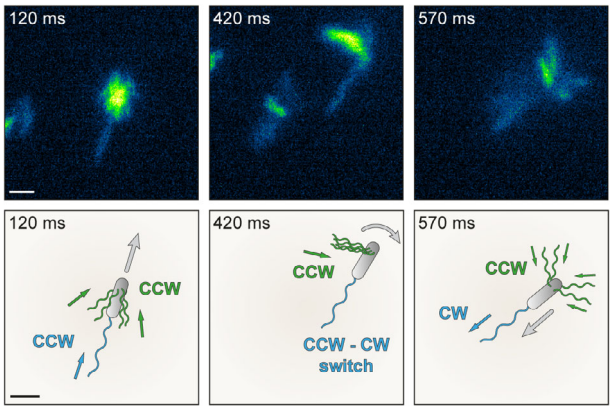

FIGURE 4 Secondary flagella may modulate turning angles during reversals induced by the primary flagellum. The figure shows snapshots of a swimming *S. putrefaciens* cell with fluorescently labelled primary and secondary flagella and corresponding cartons illustrating the micrographs. CCW, counter-clockwise. CW, clockwise. Grey arrow, overall swimming direction of the cell. Blue/green arrows, direction of flagellar propulsion. Scale bar, 2 μm. Secondary flagella (green) are always pointing towards the trailing cell pole due to viscous drag. During a reversal of swimming direction induced by the switch from CCW to CW rotation of the primary flagellum (blue) the secondary flagella can align in the same direction pointing sideways. As they constantly rotate CCW, never CW, they keep generating thrust that can induce a turn of the cell body. This turning mechanism overlays with the 'run-reverse-flick' turning mechanism controlled by the primary flagellum. This may explain why populations of cells with both flagellar systems compared to mutants with just the primary system show a different distribution of turning angles (Bubendorfer et al., 2014). Snapshots were taken from Supplementary Movie M5

secondary filaments always provided thrust in the same direction as mediated by the primary polar flagellum.

Secondary flagella affect cellular turning angles

Our data demonstrate that the secondary flagella realign as described above after a turn of the direction of swimming. This could either be induced by a reversal from pushing (forward movement) to pulling (backward movement) by the primary flagellum or a sequence of run-reverse-flick upon a switch from pulling to pushing (Son et al., 2013; Xie et al., 2011). Before and after the reversal, lateral flagella are aligned in such a way that they provide thrust in the same direction as the polar flagellum. However, during this realignment process, one or more secondary flagella will point sideways while rotating CCW, thus providing sideways thrust for a brief period of time and turning the cell body independently of the directional change induced by the primary polar flagellum [Figure 4(A), Supplementary Movie M4].

Lateral flagella and polar flagellar screw formation jointly contribute to spreading in soft agar

We previously showed that high load on the *S. putrefaciens* polar flagellum during CW rotation may induce wrapping and rotation of the flagellar filament around the cell body (Kühn et al., 2017). However, this flagellar behaviour would certainly interfere with the function of secondary lateral flagella or, vice versa, the presence of lateral filaments may inhibit flagellar wrapping and screw thread motility. For further investigation we therefore observed cells with labelled flagellar filaments on microscopic agar slides with an excess of medium that leaves channels of various widths to move between the

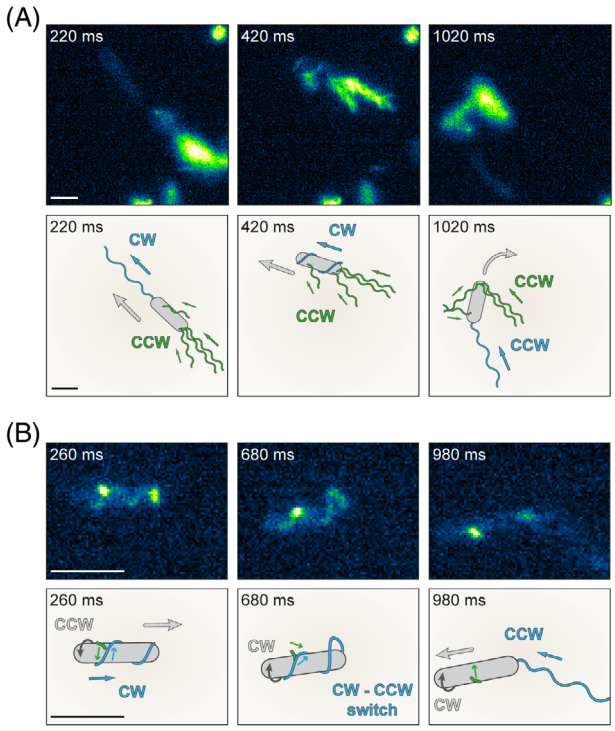

FIGURE 5 Secondary flagella do not inhibit wrapping of the primary flagellum around the cell body. The figure shows snapshots of swimming *S. putrefaciens* cells with fluorescently labelled primary and secondary flagella and corresponding cartons illustrating the micrographs. CCW, counter-clockwise. CW, clockwise. Grey arrow, overall swimming direction of the cell. Blue/green arrows, direction of flagellar propulsion. Scale bar, 2 μm. (A) The primary polar flagellum (blue) is still able to wrap around the cell body despite secondary lateral flagella (green) located on the cell surface. The secondary flagella at the trailing cell pole are likely too far away for interaction with the wrapped primary flagellum; however, the primary flagellum clearly moves over the secondary flagellum located at the side of the cell. Both flagella are rotating slowly without disturbing each other. Snapshots were taken from Supplementary Movie M6. (B) The short secondary lateral flagellum indicates the counterrotation of the cell body induced by the rotation of the primary flagellum rotating over the lateral flagellar stump while wrapped around the cell body. During the reversal of motor rotation of the primary flagellum and release of the wrapped flagellum the movement of the lateral flagellar stump indicates an inversion of the cell body counterrotation. Thus, the screw thread configuration of the primary flagellum is not disturbed by rotating over obstacles on the cell surface that are rotating in the opposite direction. Snapshots were taken from Supplementary Movie M7

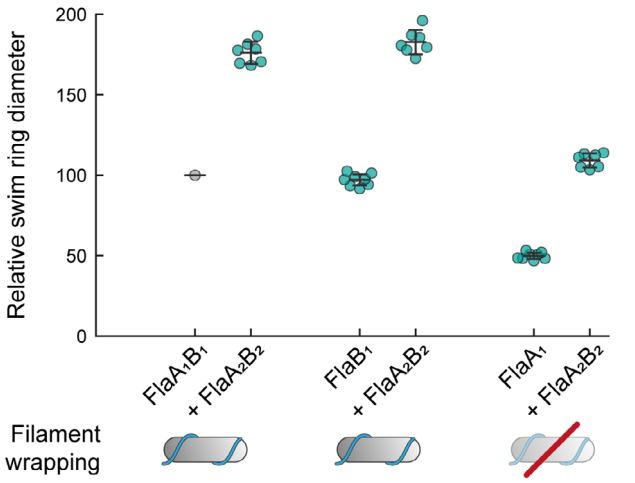

FIGURE 6 Secondary flagella and polar flagellar wrapping jointly contribute to spreading in soft agar. Radial expansion in 0.2% soft agar of mutants with just primary flagella ($FlaA_1$ and $FlaB_1$, left) or both primary and secondary flagella ($FlaA_2$ and $FlaB_2$, right). For the primary system, three mutants are shown: $FlaAB_1$, WT; $FlaB_1$, only major flagellin; $FlaA_1$, only minor flagellin expressed from the promotor of the major flagellin. The primary flagellum only composed of $FlaA_1$ is not capable of wrapping around the cell body (as indicated below the graph). Both the addition of the secondary flagella as well as the ability to wrap the filament contribute independently to the expansion speed of the colonies. All strains were tested against a mutant with only the primary flagellum ($FlaAB_1$). Representative images of the soft-agar plates are shown in Supplementary Figure 2

rough agar surface and the microscopy cover slip (Kühn et al., 2017). Using this setup, we observed that for cells pulling through narrow spaces wrapping of the polar filament was not inhibited by the presence of secondary lateral flagella (Figure 5; Supplementary Movies M5 and M6). Movement of the polar flagellar helix around the cell body occurred across lateral filaments, while secondary filaments located close to the opposite pole were unaffected and still acted as motility support and pushed the cells into the direction of movement. These observations strongly suggested that secondary lateral flagella and polar flagella wrapping are not mutually exclusive but may even jointly support motility in structured or constricted environments. To challenge this hypothesis, we compared the spreading of (i) cells lacking secondary flagella ($\Delta flaA_2B_2$), (ii) cells not able to wrap the primary polar flagellum ($FlaA_1$-only; Kühn et al., 2018) and (iii) combining both mutations to that of wild-type cells [Figure 6; Supplementary Figure 2(C)]. Loss of secondary flagella or the ability of primary flagellar wrapping each decreased the ability of the mutant cells to spread in soft agar (~60% and ~50% diameter relative to that of wild-type cells, respectively). Of note, the double mutant showed an additive defect in spreading (~30% diameter relative to that of wild-type cells). Based on the results, we concluded that secondary flagellation and the ability of polar flagellar wrapping cumulatively enhance the cells' spreading through a structured environment, such as soft agar.

DISCUSSION

As a number of bacterial species, *S. putrefaciens* possesses two distinct flagellar systems (Bubendorfer et al., 2012). In this species, the secondary system is induced in free swimming planktonic cells in complex media, which enabled us to study the behaviour of two

flagellar systems synchronously driving swimming motility.

To this end, we first characterized the composition of the secondary flagellar filaments. Generally, flagellar filaments are tube-like structures assembled from thousands of copies of the main building block flagellin (Samatey et al., 2001; Wang et al., 2017). Roughly about half of all flagellated bacterial species possess more than a single type of flagellin (Faulds-Pain et al., 2011). We previously showed that the *S. putrefaciens* primary polar flagellum is composed of two distinct flagellins, $FlaA_1$ and $FlaB_1$ (Kühn et al., 2018). Notably, filaments made from only $FlaA_1$ or $FlaB_1$ differ significantly with respect to their geometry. $FlaA_1$-only filaments are rather narrow with a high pitch while filaments consisting of only $FlaB_1$ are broader with a lower pitch, and this has pronounced effects on the properties of the filament and its ability to drive the cell through different environments (Kühn et al., 2018). In the wild-type filament the flagellins are assembled in a spatial fashion with $FlaA_1$ at the basis of the flagellum close to the cell and $FlaB_2$ forming the major section of the filament. The $FlaA_1$ segment is supposed to function as a strengthening element, which allows fast swimming but also wrapping of the flagellum around the cell body upon high load on the filament. Flagellar wrapping enables screw thread motility to escape from traps in which the cell got stuck. According to the genetic data, also the *S. putrefaciens* secondary flagellar gene cluster encodes two distinct flagellins, $FlaA_2$ and $FlaB_2$. We found that, in contrast to the primary system, both secondary flagellins are synchronously produced and are not assembled in a spatial fashion. Instead, the flagellum appears as a mixture of both flagellin types in a geometry that more closely resembles that of the polar $FlaA_1$-only filament than that of the wild-type filament of the primary system (Kühn et al., 2017, 2018). Mutants deleted in either *flaA*$_2$ or *flaB*$_2$ formed secondary filaments with a geometry that was almost indistinguishable from that of wild-type filaments as well; however, the mutant's flagellar filaments were shorter, which may be due to a lower overall amount of flagellin produced. The mixed-flagellin wild-type filament allowed a slightly better spreading performance, which did, however, not directly correlate with the average filament lengths as FlaB-only mutants had a shorter filament but were better in spreading. The more efficient spreading may therefore be based on filament properties such as stiffness or on differences in geometry too subtle to be identified by our fluorescence microscopy approach. Further advantages of the mixed-flagellin filament, e.g. in surface swarming and adhesion, overall stability, or even immune system evasion, which are functions generally discussed for lateral flagella (McCarter, 2004; Merino et al., 2006), may occur, but this remains to be shown.

In a number of bacterial species, the flagellins are modified by glycosyl groups, which are commonly attached to serine or threonine residues (O-linked), so that the whole polar filament is decorated by glycosylation (Merino et al., 2006). In the *Aeromonas* species *A. hydrophila* and *A. caviae*, which both harbour a dual flagellar system similar to that of *S. putrefaciens*, both the main polar as well as the secondary lateral flagellar filaments are glycosylated (Canals et al., 2007; Gavín et al., 2003; Rabaan et al., 2001). We previously found that the flagellins $FlaA_1$ and $FlaB_1$ of the main *S. putrefaciens* polar flagellar system are similarly modified by glycosyl groups (Kühn et al., 2018). Thus, a fully functional flagellin glycosylation machinery is present in this species. No apparent size shift of the secondary flagellins occurred in mutants lacking the polar flagellin glycosylation machinery, which may suggest that the *S. putrefaciens* secondary flagellins are not, or at least not extensively glycosylated. Glycosylation of the *Shewanella* primary flagellins occurs within the flagellin domains that are not required for flagellin stacking (the N- and C-terminal D_0 and D_1 regions; see Supplementary Figure 1), but at serine residues within the variable regions, which located between the D_0 and D_1 domains and are exposed to the environment (Bubendorfer et al., 2013; Sun et al., 2013). Notably, within *S. putrefaciens* $FlaA_2$ and $FlaB_2$, a number of threonine, but no serine residues are present in the putatively surface-exposed flagellin region that would be prone for glycosylation. The nature of the residues modified in $FlaA_1$ and $FlaB_1$ of the *S. putrefaciens* primary polar flagellum is yet unknown (Bubendorfer et al., 2013; Sun et al., 2013). While the proteins involved in flagellin glycosylation have been identified in several species, the exact mechanism underlying this process is still unsolved. However, based on our findings we hypothesize that the flagellin glycosylation machinery of *S. putrefaciens* exclusively targets serine residues or has other means to discriminate between the primary and secondary flagellins.

Synchronous fluorescent labelling of both primary and secondary *S. putrefaciens* flagellar filaments allowed insights into bacterial swimming mediated by a combination of two fundamentally different flagellar systems. The results confirmed earlier results that were based on different staining methods (Bubendorfer et al., 2012) and showed that one to five (and sometimes more) secondary filaments can be localized at various positions around the cell, including at or close to the cell pole. The *S. putrefaciens* secondary filaments are left-handed and turn in CCW direction. They appear to be rather rigid and, when not positioned close cell pole, point away from the cell surface at an angle of 30°–50° and hence did not form a trailing bundle pushing the cells. We also did not observe polymorphic transitions, i.e. changes in the geometry of the filaments. Upon switching of the swimming direction initiated by the chemotactic primary flagellum, the secondary flagella instantly flipped over (see Figure 4). During that

process the secondary flagella would also push sideways for a brief period of time, thereby modulating the turning angle of the cell. This is in agreement with the results of previous studies showing that the distribution of turning angles is different in wild-type cells having both flagellar systems compared to mutants that express only polar flagella (Bubendorfer et al., 2014). It is conceivable that this becomes even more pronounced in media with a higher viscosity or in more densely structured environments.

The observable angle between cell surface and lateral filaments may be due to the properties of the lateral flagellar hook, the universal joint that connects filament and the rotary motor in the cell envelope (Imada, 2018). However, it is unclear if length of the hook, its structure, or both play a role in restricting the margin of manoeuvre for the secondary filament. In contrast, when secondary filaments were located close to the lagging cell pole with respect to the swimming direction, they came in close proximity in a structure with a bundle-like appearance. This potential bundle fell apart when the cell switched direction. In addition, activity of lateral flagella resulted in a rotation of the cell body, which was observed to occur both in CCW and CW direction also in cells with a stalled or lacking polar flagellum. Whether this rotation is of any physiological relevance is not clear.

So far, due to lack of comparable data it remains elusive if our findings also relate to other species with two flagellar systems. A study on the swimming behaviour of *Bradyrizobium diazoefficiens*, a species also expressing two distinct flagellar systems during planktonic swimming, indicated that the secondary lateral flagella also do not generally form a bundle (Quelas et al., 2016). However, this hypothesis was deduced from the observed swimming pattern and not from microscopic visualization of the filaments.

Our study also indicates that flagellar wrapping of the polar flagellum around the cell body, which enables screw thread motility that is highly beneficial in constricted environments (Kühn et al., 2017, 2018), is not generally inhibited by the presence of lateral flagella. In contrast, our observations strongly suggest that the polar flagellum is able to wrap and rotate over lateral secondary filaments. These jammed filaments are unlikely to contribute to motility as long as screw thread motility proceeds. However, secondary filaments located close to the opposite cell pole are not affected by the wrapped polar flagellum. Therefore, they are still able to push the cell in the direction of movement and may therefore help to release a cell trapped in a narrow confinement. It is also conceivable that during movement through a polysaccharide matrix, as in soft-agar plates, rotation of rigid filaments protruding from the cell body in an angular fashion may also facilitate propulsion through direct contact with the substratum. Both hypotheses are in accordance with our finding that flagellar wrapping and lateral flagellar jointly accelerate motility through structured environments, such as soft agar.

Taken together, we show here that the *S. putrefaciens* secondary flagella do not only act as an effective helper system during free swimming, e.g. by lowering the turning angles to increase the directional persistence (Bubendorfer et al., 2014). The additional flagella also assist the cell when moving through structured environments or to release itself when trapped in narrow passages. However, as assembly and operation of flagella are metabolically expensive, *S. putrefaciens* restricts formation of lateral flagella to a subpopulation of the cells only under appropriate environmental conditions. We found that regulation of formation and activity of the secondary flagella at least partially depends on c-di-GMP levels (Pecina et al., 2021; Rossmann et al., 2019), and further studies are directed at the question of how environmental signals are translated into the activation of the secondary system.

ACKNOWLEDGEMENTS

The work was supported by grants from the Deutsche Forschungsgemeinschaft (TH 831/6-1 and TH 831/8-1). Open Access funding enabled and organized by Projekt DEAL.

CONFLICT OF INTEREST

The authors declare no conflict of interest.

DATA AVAILABILITY STATEMENT

The authors confirm that the data supporting the findings of this study are available within the article and its supplementary materials. Further data are available upon reasonable request to the corresponding author.

ORCID

Kai M. Thormann https://orcid.org/0000-0001-7292-4884

REFERENCES

Berg, H.C. (2004) *E. coli in motion*. New York: Springer-Verlag.

Bi, S. & Sourjik, V. (2018) Stimulus sensing and signal processing in bacterial chemotaxis. *Current Opinion in Microbiology*, 45, 22–29.

Biquet-Bisquert, A., Labesse, G., Pedaci, F. & Nord, A.L. (2021) The dynamic ion motive force powering the bacterial flagellar motor. *Frontiers in Microbiology*, 12, 659464.

Bubendorfer, S., Held, S., Windel, N., Paulick, A., Klingl, A. & Thormann, K.M. (2012) Specificity of motor components in the dual flagellar system of *Shewanella putrefaciens* CN-32. *Molecular Microbiology*, 83, 335–350.

Bubendorfer, S., Ishihara, M., Dohlich, K., Heiss, C., Vogel, J., Sastre, F. et al. (2013) Analyzing the modification of the *Shewanella oneidensis* MR-1 flagellar filament. *PLoS One*, 8, e73444.

Bubendorfer, S., Koltai, M., Rossmann, F., Sourjik, V. & Thormann, K. M. (2014) Secondary bacterial flagellar system improves bacterial spreading by increasing the directional persistence of swimming. *Proceedings of the National Academy of Sciences of the United States of America*, 111, 11485–11490.

Canals, R., Vilches, S., Wilhelms, M., Shaw, J.G., Merino, S. & Tomás, J.M. (2007) Non-structural flagella genes affecting both polar and lateral flagella-mediated motility in *Aeromonas hydrophila*. *Microbiology*, 153, 1165–1175.

Chevance, F.F.V. & Hughes, K.T. (2008) Coordinating assembly of a bacterial macromolecular machine. *Nature Reviews Microbiology*, 6, 455–465.

Chu, J., Liu, J. & Hoover, T.R. (2020) Phylogenetic distribution, ultrastructure, and function of bacterial flagellar sheaths. *Biomolecules*, 10, 363.

Faulds-Pain, A., Birchall, C., Aldridge, C., Smith, W.D., Grimaldi, G., Nakamura, S. et al. (2011) Flagellin redundancy in *Caulobacter crescentus* and its implications for flagellar filament assembly. *Journal of Bacteriology*, 193, 2695–2707.

Fenchel, T. (2002) Microbial behavior in a heterogeneous world. *Science*, 296, 1068–1071.

Gautheret, D. & Lambert, A. (2001) Direct RNA motif definition and identification from multiple sequence alignments using secondary structure profiles. *Journal of Molecular Biology*, 313, 1003–1011.

Gavín, R., Merino, S., Altarriba, M., Canals, R., Shaw, J.G. & Tomás, J.M. (2003) Lateral flagella are required for increased cell adherence, invasion and biofilm formation by Aeromonas spp. *FEMS Microbiology Letters*, 224, 77–83.

Gibson, D.G., Young, L., Chuang, R.-Y., Venter, J.C., Hutchison, C. A. & Smith, H.O. (2009) Enzymatic assembly of DNA molecules up to several hundred kilobases. *Nature Methods*, 6, 343–345.

Imada, K. (2018) Bacterial flagellar axial structure and its construction. *Biophysical Reviews*, 10, 559–570.

Jarrell, K.F. & McBride, M.J. (2008) The surprisingly diverse ways that prokaryotes move. *Nature Reviews Microbiology*, 6, 466–476.

Jiang, Z.Y., Rushing, B.G., Bai, Y., Gest, H. & Bauer, C.E. (1998) Isolation of *Rhodospirillum centenum* mutants defective in phototactic colony motility by transposon mutagenesis. *Journal of Bacteriology*, 180, 1248–1255.

Kanbe, M., Yagasaki, J., Zehner, S., Göttfert, M. & Aizawa, S.-I. (2007) Characterization of two sets of subpolar flagella in *Bradyrhizobium japonicum*. *Journal of Bacteriology*, 189, 1083–1089.

Kawagishi, I., Maekawa, Y., Atsumi, T., Homma, M. & Imae, Y. (1995) Isolation of the polar and lateral flagellum-defective mutants in *Vibrio alginolyticus* and identification of their flagellar driving energy sources. *Journal of Bacteriology*, 177, 5158–5160.

Kearns, D.B. (2010) A field guide to bacterial swarming motility. *Nature Reviews Microbiology*, 8, 634–644.

Kühn, M.J., Schmidt, F.K., Eckhardt, B. & Thormann, K.M. (2017) Bacteria exploit a polymorphic instability of the flagellar filament to escape from traps. *Proceedings of the National Academy of Sciences of the United States of America*, 114, 6340–6345.

Kühn, M.J., Schmidt, F.K., Farthing, N.E., Rossmann, F.M., Helm, B., Wilson, L.G. et al. (2018) Spatial arrangement of several flagellins within bacterial flagella improves motility in different environments. *Nature Communications*, 9, 5369.

Laemmli, U.K. (1970) Cleavage of structural proteins during the assembly of the head of bacteriophage T4. *Nature*, 227, 680–685.

Lassak, J., Bubendorfer, S. & Thormann, K.M. (2013) Domain analysis of ArcS, the hybrid sensor kinase of the *Shewanella oneidensis* MR-1 Arc two-component system, reveals functional differentiation of its two receiver domains. *Journal of Bacteriology*, 195, 482–492.

Macke, T.J., Ecker, D.J., Gutell, R.R., Gautheret, D., Case, D.A. & Sampath, R. (2001) RNAMotif, an RNA secondary structure definition and search algorithm. *Nucleic Acids Research*, 29, 4724–4735.

McCarter, L.L. (2004) Dual flagellar systems enable motility under different circumstances. *Journal of Molecular Microbiology and Biotechnology*, 7, 18–29.

McClain, J., Rollo, D.R., Rushing, B.G. & Bauer, C.E. (2002) *Rhodospirillum centenum* utilizes separate motor and switch components to control lateral and polar flagellum rotation. *Journal of Bacteriology*, 184, 2429–2438.

Merino, S. & Tomás, J.M. (2014) Gram-negative flagella glycosylation. *International Journal of Molecular Sciences*, 15, 2840–2857.

Merino, S., Shaw, J.G. & Tomás, J.M. (2006) Bacterial lateral flagella: an inducible flagella system. *FEMS Microbiology Letters*, 263, 127–135.

Najafi, J., Shaebani, M.R., John, T., Altegoer, F., Bange, G. & Wagner, C. (2018) Flagellar number governs bacterial spreading and transport efficiency. *Science Advances*, 4, eaar6425.

Nakamura, S. & Minamino, T. (2019) Flagella-driven motility of bacteria. *Biomolecules*, 9, 279.

Pecina, A., Schwan, M., Blagotinsek, V., Rick, T., Klüber, P., Leonhard, T. et al. (2021) The stand-alone PilZ-domain protein MotL specifically regulates the activity of the secondary lateral flagellar system in *Shewanella putrefaciens*. *Frontiers in Microbiology*, 12, 668892.

Quelas, J.I., Althabegoiti, M.J., Jimenez-Sanchez, C., Melgarejo, A. A., Marconi, V.I., Mongiardini, E.J. et al. (2016) Swimming performance of *Bradyrhizobium diazoefficiens* is an emergent property of its two flagellar systems. *Scientific Reports*, 6, 23841.

Rabaan, A.A., Gryllos, I., Tomás, J.M. & Shaw, J.G. (2001) Motility and the polar flagellum are required for *Aeromonas caviae* adherence to HEp-2 cells. *Infection and Immunity*, 69, 4257–4267.

Reichenbach, T., Mobilia, M. & Frey, E. (2007) Mobility promotes and jeopardizes biodiversity in rock–paper–scissors games. *Nature*, 448, 1046–1049.

Rossmann, F.M., Rick, T., Mrusek, D., Sprankel, L., Dörrich, A.K., Leonhard, T. et al. (2019) The GGDEF domain of the phosphodiesterase PdeB in *Shewanella putrefaciens* mediates recruitment by the polar landmark protein HubP. *Journal of Bacteriology*, 201, e00534-18.

Samatey, F.A., Imada, K., Nagashima, S., Vonderviszt, F., Kumasaka, T., Yamamoto, M. et al. (2001) Structure of the bacterial flagellar protofilament and implications for a switch for supercoiling. *Nature*, 410, 331–337.

Schindelin, J., Arganda-Carreras, I., Frise, E., Kaynig, V., Longair, M., Pietzsch, T. et al. (2012) Fiji: an open-source platform for biological-image analysis. *Nature Methods*, 9, 676–682.

Schuhmacher, J.S., Thormann, K.M. & Bange, G. (2015) How bacteria maintain location and number of flagella? *FEMS Microbiology Reviews*, 39, 812–822.

Shimada, T., Sakazaki, R. & Suzuki, K. (1985) Peritrichous flagella in mesophilic strains of Aeromonas. *Japanese Journal of Medical Science & Biology*, 38, 141–145.

Shinoda, S. & Okamoto, K. (1977) Formation and function of *Vibrio parahaemolyticus* lateral flagella. *Journal of Bacteriology*, 129, 1266–1271.

Son, K., Guasto, J.S. & Stocker, R. (2013) Bacteria can exploit a flagellar buckling instability to change direction. *Nature Physics*, 9, 494–498.

Song, W., Maiste, P.J., Naiman, D.Q. & Ward, M.J. (2007) Sigma 28 promoter prediction in members of the Gammaproteobacteria. *FEMS Microbiology Letters*, 271, 222–229.

Song, W., Juhn, F.S., Naiman, D.Q., Konstantinidis, K.T., Gardner, T. S. & Ward, M.J. (2008) Predicting sigma28 promoters in eleven *Shewanella* genomes. *FEMS Microbiology Letters*, 283, 223–230.

Sourjik, V. & Wingreen, N.S. (2012) Responding to chemical gradients: bacterial chemotaxis. *Current Opinion in Cell Biology*, 24, 262–268.

Sun, L., Jin, M., Ding, W., Yuan, J., Kelly, J. & Gao, H. (2013) Post-translational modification of flagellin FlaB in *Shewanella oneidensis*. *Journal of Bacteriology*, 195, 2550–2561.

Thormann, K.M., Beta, C. & Kühn, M.J. (2022) Wrapped up: The motility of polarly flagellated bacteria. *Annual Review of Microbiology*, 76, 1.

Tinevez, J.-Y., Perry, N., Schindelin, J., Hoopes, G.M., Reynolds, G. D., Laplantine, E. et al. (2017) TrackMate: An open and extensible platform for single-particle tracking. *Methods*, 115, 80–90.

Wadhwa, N. & Berg, H.C. (2021) Bacterial motility: machinery and mechanisms. *Nature Reviews Microbiology*, 20, 161–173.

Wang, F., Burrage, A.M., Postel, S., Clark, R.E., Orlova, A., Sundberg, E.J. et al. (2017) A structural model of flagellar filament switching across multiple bacterial species. *Nature Communications*, 8, 960.

Xie, L., Altindal, T., Chattopadhyay, S. & Wu, X.-L. (2011) Bacterial flagellum as a propeller and as a rudder for efficient chemotaxis. *Proceedings of the National Academy of Sciences of the United States of America*, 108, 2246–2251.

SUPPORTING INFORMATION

Additional supporting information can be found online in the Supporting Information section at the end of this article.

How to cite this article: Kühn, M.J., Edelmann, D.B. & Thormann, K.M. (2022) Polar flagellar wrapping and lateral flagella jointly contribute to *Shewanella putrefaciens* environmental spreading. *Environmental Microbiology*, 1–13. Available from: https://doi.org/10.1111/1462-2920.16107